



M_W helps select Z' models for $b \rightarrow s\ell\ell$ anomalies

Ben Allanach^{1,a}, Joe Davighi^{2,b}

¹ DAMTP, University of Cambridge, Wilberforce Road, Cambridge CB3 0WA, UK

² Physik-Institut, Universität Zürich, 8057 Zurich, Switzerland

Received: 7 June 2022 / Accepted: 9 August 2022 / Published online: 24 August 2022
 © The Author(s) 2022

Abstract As shown in Allanach et al. (Global fits of third family hypercharge models to neutral current B-anomalies and electroweak precision observables. [arXiv:2103.12056](https://arxiv.org/abs/2103.12056)), the Third Family Hypercharge (Y_3) Model changes the Standard Model prediction for M_W whilst simultaneously explaining anomalies in $b \rightarrow s\ell\ell$ transitions via a heavy Z' gauge boson which is spawned by a spontaneously broken gauged $U(1)_{Y_3}$ symmetry. The 2022 CDF II measurement of M_W , which is far from the Standard Model prediction in the statistical sense, somewhat disfavours the Y_3 model. Here, we generalise the gauge charge assignments to the anomaly-free combination $sY_3 + t(B_3 - L_3)$ and show that incorporating the 2022 CDF II measurement of M_W selects a viable domain of integers s and t . For example, $s = 1, t = -3$ yields a p value of .08 in a two-parameter global fit to 277 electroweak and flavour changing b data, much improving a SM p value of 1×10^{-6} .

1 Introduction

Recently, the CDF II Collaboration reported a measurement of the W boson mass $M_W = 80.4335 \pm 0.0094$ GeV [2] that disagrees by many sigma with the Standard Model (SM) prediction of the quantity. One average¹ of all current measurements yields [4]

$$M_W = 80.4133 \pm 0.0080 \text{ GeV}, \quad (1.1)$$

still in significant disagreement (with a pull of -6.4σ) with SM predictions; we call this disagreement the M_W anomaly. Note that the top quark mass m_t plays an important role in the prediction of M_W in the SM: throughout this paper, we impose the following constraint upon the top quark pole mass,

$$m_t = 171.79 \pm 0.38 \text{ GeV}, \quad (1.2)$$

based on a combination of the latest data [4]. We use the `smelli2.3.2` defaults [5] for other electroweak constraints and parameters.

There are also discrepancies between SM predictions and some measurements of flavour-changing B -meson decays, which we collectively call the $b \rightarrow s\ell\ell$ anomalies. For example, various lepton flavour universality (LFU) observables like the ratios of branching ratios $R_{K^{(*)}} = BR(B \rightarrow K^{(*)}\mu^+\mu^-)/BR(B \rightarrow K^{(*)}e^+e^-)$ are observed to be lower than their SM predictions in several channels and several different bins of di-lepton invariant mass squared [6–8]. Similar double ratio measurements in $B^0 \rightarrow K_s^0\ell^+\ell^-$ and $B^+ \rightarrow K^{*+}\ell^+\ell^-$ decays [9] are consistent with a similar deficit in di-muons over di-electrons, albeit with lower statistics than in $R_{K^{(*)}}$. The predictions for all aforementioned double ratios have rather small theoretical uncertainties due to cancellations and the SM predictions are generically considered to be

Contents

1 Introduction	1
2 The models	3
2.1 Symmetry breaking and $Z - Z'$ mixing	4
2.2 Fermion mixing matrices	4
3 SMEFT matching	5
4 Phenomenology	5
4.1 Important observables	5
Electroweak	5
$b \rightarrow s\ell\ell$	6
4.2 Global fits	7
5 Conclusions	8
References	10

^a e-mail: B.C.Allanach@damtp.cam.ac.uk

^b e-mail: joe.davighi@physik.uzh.ch (corresponding author)

¹ For an electroweak fit in terms of S, T and U parameters, see Ref. [3].

robust in the di-lepton invariant mass squared bins of interest. $BR(B_s \rightarrow \mu^+ \mu^-)$ also has quite small theoretical uncertainties in its SM prediction. The combined measurements of $BR(B_s \rightarrow \mu^+ \mu^-)$ are in a 2σ tension with its SM prediction [10–14]. Several other B -meson decay observables appear to be in tension with SM predictions even when their larger theoretical uncertainties are taken into account: for example angular distributions in $B \rightarrow K^* \mu^+ \mu^-$ decays [15–20], and $BR(B_s \rightarrow \phi \mu^+ \mu^-)$ [21,22]. For these quantities though, there is room for argument about the assumed size of the theoretical uncertainties and indeed the best way of estimating the SM predictions for them.

We display the statistical tensions in the SM due to the M_W and $b \rightarrow s\ell\ell$ anomalies in Table 1, as calculated by the computer program² `smelli2.3.2` [5]. We see from the table that the $b \rightarrow s\ell\ell$ anomalies disfavour the SM: the $b \rightarrow s\ell\ell$ data yields a poor fit with a global p value of .0036, even when using the default `smelli2.3.2` constraints upon the EWPOs (4.13), i.e. *excluding* the new CDF II measurement of M_W (although the EWPOs have an acceptable fit in and of themselves with a p value of .17). Taking into account the CDF II measurement of M_W as in (1.1) exacerbates an already poor quality of fit, lowering the global p value to 10^{-6} .

Global fits find that new physics contributions to the $(\bar{b}\gamma^\mu P_L s)(\bar{\mu}\gamma_\mu P_X \mu) + H.c.$ vertex in the Lagrangian density can ameliorate the fit to the $b \rightarrow s\ell\ell$ data [23–29], where P_L is the left-handed projection operator. P_X corresponds to the helicity projection of the muon pair in the effective vertex: the fits agree that a purely right-handed projection $P_X = P_R$ is disfavoured, whereas a mixture in the domain $P_X \approx P_L$ to $P_X \approx P_L + P_R$ is preferred [30]. Whereas the fitting groups yield very similar results when fitting just to the ‘LFU’ category of observables, there are some differences observed when the ‘quarks’ category is included: for example, which option out of $P_X = P_L$ or $P_X = P_L + P_R$ has a better fit. Such differences in the constraints can arise from the treatment of theoretical uncertainties in the ‘quarks’ category. The lesson one learns from such studies is that, from a new physics point of view in order to fit the $b \rightarrow s\ell\ell$ anomalies, one needs a new physics state that couples to left-handed quark fields and left-handed muon fields in a family non-universal manner (but it may or may not also couple to right-handed muon fields and/or electron fields). According to Ref. [31], there is a mild preference for a family universal coupling of new physics to leptons as well as a specific and different new physics contribution to the coupling to di-muon pairs.

One category of new physics state that can have such couplings is a heavy electrically-neutral vector boson, dubbed a Z' [32–36]. In specific models, one obtains the Z' from

a spontaneously broken additional $U(1)_X$ gauge symmetry under which the SM fermions have family dependent charges. In a consistent ultra-violet (UV) complete model, quantum field theoretic anomalies should cancel.³ Our model here will not be UV complete, since new physics above the TeV scale is required to generate the light Yukawa couplings (once integrated out and matched onto our $SM \times U(1)_X$ model). Nevertheless, it is wise to cancel gauge anomalies in the $SM \times U(1)_X$ model, as we do here; if not, there must be heavy chiral fermions to cancel anomalies, whose masses are at least tied to the TeV-scale $U(1)_X$ breaking. Many viable anomaly-free $U(1)_X$ charge assignments have been investigated: for example muon minus tau lepton number [41–46], third family baryon number minus second family lepton number [47–49], third family hypercharge [50–52] or other assignments [53–72].

In Ref. [50], the Third Family Hypercharge (Y_3) model was presented and shown to fit the $b \rightarrow s\ell\ell$ data. Here, the X charges of all fermions are zero except for the third family, which has X charge equal to its hypercharge. The model predicts $Z - Z'$ mixing because the Higgs doublet is necessarily charged under $U(1)_X$ to allow a renormalisable top Yukawa coupling, which would otherwise be forbidden by the $U(1)_X$ gauge symmetry. It was noted that this will change the SM prediction for M_W [73] and in Ref. [1] it was shown that the model could simultaneously fit the $b \rightarrow s\ell\ell$ anomalies and EWPOs: indeed, that the SM prediction for M_W was improved, since it was some 2σ too low in the SM (compared to the measurement at the time) but receiving a positive correction from the Y_3 model.

We will show below that including the new CDF II measurement of M_W as in (1.1), the Y_3 model is somewhat disfavoured with a global p value of .02. Our purpose in this paper is then to build a generalisation of the Y_3 model, which is similar in construction and as simple, but which provides a simultaneously acceptable fit to both the M_W anomaly and $b \rightarrow s\ell\ell$ anomalies. To this end, in Sect. 2, we shall propose a generalisation of the Y_3 charge assignments, which is rendered anomaly-free simply by the inclusion of right-handed neutrinos. There are two classes of charge assignment, depending upon whether one permutes the *right-handed* third family field’s charged lepton charge with that of the second family (i.e. $X_{e_3} \leftrightarrow X_{e_2}$) or not. In Sect. 3, we calculate the SM effective field theory (SMEFT) coefficients that arise from integrating out the heavy Z' boson, and then matching to the SMEFT at tree level. This allows us to encode

² We use the development version of `smelli2.3.2` and its sub-program `flavio2.3.3` that were on github on 27/4/22.

³ The equations for cancellation of local gauge anomalies have been solved analytically for a gauge group of the form $SM \times U(1)_X$ [37], although it is often easiest to search lists to identify anomaly-free charge assignments of phenomenological interest [38]. It has also been shown [39] that a $SM \times U(1)_X$ gauge theory suffers from no global gauge anomalies provided only that the $SU(2)_L$ anomaly [40] cancels, as it does here.

Table 1 SM goodness of fit as calculated by `smelli2.3.2`. n_{obs} shows the number of observables in each category.

Category	n_{obs}	χ^2	p	p (global)	Pull (M_W)
Quarks	224	269	.021		
LFU FCNCs	23	39.4	.018		
EWPOs (<code>smelli</code>)	31 s	38.4	.17	.0036	−2.1
EWPOs (CDF II)	30	93.6	2.9×10^{-6}	1.3×10^{-6}	−6.4

χ^2 denotes the χ^2 statistic within that category, p is the p value of the category, and $p(\text{global})$ is the global p value of all observables. The category ‘LFU FCNCs’ contains lepton flavour universality violating flavour changing observables such as $R_K^{(*)}$ as well as $BR(B_s \rightarrow \mu^+ \mu^-)$, where theoretical uncertainties are relatively small. The ‘quarks’ category contains other flavour-changing b observables, some of which have large theoretical uncertainties. The category EWPOs (`smelli`) contains electroweak precision observables for the default `smelli2.3.2` combination of M_W (4.13) which excludes the CDF II measurement, whereas EWPOs(CDF II) includes it in a global average à la (1.1), (1.2). $p(\text{global})$ includes the ‘quarks’ category, the ‘LFU FCNCs’ category and the ‘EWPO’ category relevant for the respective combination of M_W measurements. For a definition of the pull, see (4.14) and the discussion of it in the surrounding text

our model in a suitable form for input into `smelli2.3.2` and use its calculation of EWPOs, LFU observables and the ‘quarks’ category of observables. We discuss the phenomenology of the models in Sect. 4, in particular the effect on M_W and on $b \rightarrow s \ell \ell$ coefficients in the weak effective theory. The case where one permutes $X_{e_3} \leftrightarrow X_{e_2}$ corresponds to $P_X = P_L + P_R$, whereas in the case where one does not, one obtains a certain linear combination of P_L and P_R , depending upon s and t . In both cases, there is a purely axial coupling to electrons. We then present global fits to this latter family of model. The inclusion of the 2022 CDF II M_W measurement selects a subset of models which provide acceptable fits to the collective data. We conclude in §5.

2 The models

We consider a class of Z' models based on extending the SM gauge symmetry by a $U(1)_X$ factor, where

$$X = sY_3 + t(B - L)_3, \quad s \in \mathbb{N}, t \in \mathbb{Z}, \quad (2.1)$$

Y_3 is third family hypercharge and $(B - L)_3$ is third family baryon number minus lepton number. Our conventions for the representations of the non-gauge fields in the model are shown in Table 2.

The X charge assignment in (2.1) is the most general anomaly-free $U(1)_X$ extension⁴ that couples only to a single family of SM fermions [38], including a right-handed neutrino. While we have parameterised this family of $U(1)_X$ models by two integers s and t , it is only the rational parameter $t/s \in \mathbb{Q}$ that is relevant for phenomenology.⁵ This family of $U(1)_X$ extensions of the SM are known to have semi-

simple gauge completions without needing any extra chiral fermions, as was shown in Ref. [74].

The Z' model is designed to explain the $b \rightarrow s \ell \ell$ anomalies. Global fits strongly favour a lepton flavour non-universal coupling of the Z' to left-handed muons, at least, as described in Sect. 1. We thus permute the non-zero left-handed lepton charge from the third to the second family, as in the original Y_3 model of [50]. Regarding right-handed leptons, acceptable fits can be obtained with or without permuting the non-zero right-handed lepton charge to the second family.

In summary, the charges of the SM fermions, together with the SM Higgs doublet $H = (H^+, H^0)^T$ and an extra $U(1)_X$ symmetry-breaking scalar θ which is a SM singlet, are

$$X_{q_3} = s + t, \quad X_{\ell_2} = -3s - 3t, \quad (2.2)$$

$$X_{u_3} = 4s + t, \quad X_{e_n} = -6s - 3t, \quad n = 2 \text{ or } 3, \quad (2.3)$$

$$X_{d_3} = -2s + t, \quad X_{\nu_n} = -3t, \quad (2.4)$$

$$X_H = 3s, \quad X_\theta, \quad (2.5)$$

where $X_\theta \neq 0$, with all other $U(1)_X$ charges being zero. The original Y_3 model of Ref. [50], which is a template for the family of models we consider here, can be recovered by setting $n = 3$ and $(s, t) = (1, 0)$, thus decoupling the right-handed neutrino.

Like the Y_3 model [50], the family of models we consider here allow, on the quark side, only third family Yukawa couplings to the Higgs at the renormalisable level, $\mathcal{L} \supset y_t \bar{q}_3^c H^c u'_3 + y_b \bar{q}_3^c H d'_3$. Thus, to zeroth order, gauging the anomaly-free chiral third-family symmetry (2.5) postdicts a heavy third family and small quark mixing angles, as observed. The light quark Yukawa couplings, responsible for the masses of the first and second generation and for the quark mixing angles, must come from higher-dimensional operators. Such operators can come from integrating out heavier fermionic representations that are vector-like under to the gauge group. These are details of the UV theory which it

⁴ We ignore possible discrete quotients of the gauge group because they are not relevant to our discussion.

⁵ This is because all charges may be scaled by an overall factor, so long as the $U(1)_X$ gauge coupling g_X is scaled by one over this factor, with no change to the physics.

Table 2 Representations of fields under the SM gauge factors, which are family universal, together with the family non-universal Y_3 and $(B-L)_3$ symmetries on which our Z' model is based.

	$q'_1 q'_2 q'_3$	$u'_1 u'_2 u'_3$	$d'_1 d'_2 d'_3$	$\ell'_1 \ell'_2 \ell'_3$	$e'_1 e'_2 e'_3$	$\nu'_1 \nu'_2 \nu'_3$	H	θ
SU(3)	3	3	3	1	1	1	1	1
SU(2)	2	1	1	2	1	1	2	1
$U(1)_Y$	1	4	-2	-3	-6	0	3	0
$U(1)_{Y_3}$	0 0 1	0 0 4	0 0 -2	0 0 -3	0 0 -6	0 0 0	3	*
$U(1)_{(B-L)_3}$	0 0 1	0 0 1	0 0 1	0 0 -3	0 0 -3	0 0 -3	0	*

We use the minimal integer normalisation for the charges under each $U(1)$ factor. Note that the permutations $\ell_2 \leftrightarrow \ell_3$ (and in some cases $e_2 \leftrightarrow e_3$) are made *after* the assignments shown. All fields are Weyl fermions except for the complex scalar Higgs doublet H and the complex scalar flavon θ . * denotes that the charge is a non-zero number whose value does not change any of the discussion or results of this paper

would be premature to specify (although see Ref. [1] for further comments and ideas).

On the other hand, the lepton sector is not so natural from the Yukawa perspective, due to the fact that we permute the non-zero X_{ℓ_i} charge into the second family. At face value, the charge assignment (2.5) with $n = 3$ allows only for a renormalisable off-diagonal Yukawa coupling $\sim \bar{\ell}'_2 H e'_3$, which must be highly suppressed in order to explain the relative heaviness of the tau and the non-observation of $\mu - \tau$ lepton flavour violation. This is easily explained with a little more model-building; for example, additionally gauging an anomaly-free lepton-flavoured $U(1)$ symmetry could ban this off-diagonal Yukawa coupling.⁶

In what follows we use a convention in which the covariant derivative acting on a field f is

$$D_\mu = \partial_\mu - ig \frac{\sigma^a}{2} P_L W_\mu^a - ig' Y_f B_\mu - ig_X X_f X_\mu, \quad (2.6)$$

where X_μ is the gauge field for $U(1)_X$ and g_X is its gauge coupling. We assume that any kinetic mixing between $U(1)_X$ and $U(1)_Y$ gauge fields is negligible, leaving a study of such effects to future work. The fermion couplings to the gauge fields, in the gauge eigenbasis (indicated by ‘primes’), are

$$\mathcal{L}_\psi = g_X X_\mu \sum_\psi X_\psi \bar{\psi}' \gamma^\mu \psi', \quad (2.7)$$

where the sum on ψ runs over all SM Weyl fermions and the charges X_ψ are those in (2.5).

2.1 Symmetry breaking and $Z - Z'$ mixing

The $U(1)_X$ symmetry is broken predominantly by the SM singlet scalar field θ , which acquires a vacuum expectation value $\langle \theta \rangle = v_X / \sqrt{2}$, where $v_X \gg v$ is of order the TeV scale.

⁶ Another route is to look for anomaly-free deformations of (2.5) in which two families of leptons are charged, generalising [52], which allow either no renormalisable lepton Yukawa couplings, or at most the $y_\tau \bar{\ell}'_3 H e'_3$ coupling.

This implies that the mass of the Z' field $M_{Z'} \approx g_X X_\theta v_X$. However, because the SM Higgs is also charged under $U(1)_X$, there is mass mixing between the Z boson and the Z' gauge boson. These physical gauge bosons are linear combinations of the SM combination⁷ $Z_\mu^0 = c_w W_\mu^3 - s_w B_\mu$ (where $\theta_w = \tan^{-1}(g'/g)$ is the Weinberg angle) and the X_μ field viz.

$$\begin{pmatrix} Z_\mu \\ Z'_\mu \end{pmatrix} = \begin{pmatrix} c_z & s_z \\ -s_z & c_z \end{pmatrix} \begin{pmatrix} Z_\mu^0 \\ X_\mu \end{pmatrix}, \quad (2.8)$$

where the mixing angle α_z is determined by, at tree-level,

$$\sin \alpha_z = \frac{X_H g/c_w}{2X_\theta^2 g_X} \frac{v^2}{v_X^2} = \frac{2X_H g_X}{g/c_w} \frac{M_Z^2}{M_{Z'}^2} \left[1 + \mathcal{O}\left(\frac{M_Z^2}{M_{Z'}^2}\right) \right], \quad (2.9)$$

where

$$M_Z^2 = v^2 g^2 / 4c_w^2 \left[1 + \mathcal{O}\left(\frac{M_Z^2}{M_{Z'}^2}\right) \right]. \quad (2.10)$$

At a constant value of M_Z (we shall take M_Z to be an experimental input), the $\mathcal{O}(M_Z^2/M_{Z'}^2)$ correction in (2.10) translates to an upward shift in the SM prediction for M_W , as we shall describe in Sect. 4.1.

2.2 Fermion mixing matrices

Following Refs. [1, 50], we assume a simple ansatz for the 3-by-3 unitary fermion mixing matrices describing the change from the gauge eigenbasis to the (unprimed) mass eigenbasis of the fermionic fields. The purpose of this ansatz is to characterise the main physical flavour characteristics of the model without introducing large flavour-changing neutral currents that would be subject to strong experimental

⁷ We define $c_x := \cos x$, $s_x := \sin x$ throughout this paper, for various quantities x .

constraints. We may think of the ansatz as a limit to expand around: the fairly strong assumptions might be motivated by further model-building involving additional symmetries or dynamics, but we leave such considerations to one side, for now.

For left-handed down-type quarks, we parameterise the mixing matrix as

$$V_{dL} = \begin{pmatrix} 1 & 0 & 0 \\ 0 & \cos \theta_{sb} & \sin \theta_{sb} \\ 0 & -\sin \theta_{sb} & \cos \theta_{sb} \end{pmatrix}. \quad (2.11)$$

For simplicity, and to avoid unwanted large contributions to $\Delta F = 2$ processes and charged lepton flavour violating processes, we choose $V_{dR} = 1$, $V_{uR} = 1$ and $V_{eL} = 1$. Finally, $V_{uL} = V_{dL} V^\dagger$ and $V_{\nu L} = V_{eL} U^\dagger$ are fixed by the CKM matrix V and the PMNS matrix U , respectively. We use the central values of extracted angles and phases from the Particle Data Group [75].

Using these rotation matrices, the couplings of the Z' boson to the physical fermion states can be obtained from (2.7). For the left-handed quarks, we work in a ‘down-aligned’ basis in which the (unprimed) quark doublets are $q_i = (V_{ij}^\dagger u_{L,j}, d_{L,i})$. For the left-handed leptons, we work in a basis in which the left-handed charged leptons e_{Li} align with the mass eigenstates, and thus the (unprimed) lepton doublets are $\ell_i = (U_{ij}^\dagger \nu_{L,j}, e_{L,i})$. Since $V_{eL} = V_{eR} = 1$ the charged lepton couplings remain diagonal. The down quark couplings are mixed away from the diagonal, however, as is indeed necessary to obtain a quark flavour-violating coupling of the Z' to $b\bar{s}$ and $\bar{s}b$. We have:

$$\mathcal{L}_\psi \supset g_X X_\mu (X_{q3} \Lambda_{ij}^{dL} \bar{q}_i \gamma^\mu q_j + X_{u3} \bar{u}_3 \gamma^\mu u_3 + X_{d3} \bar{d}_3 \gamma^\mu d_3 + X_{\ell 2} \bar{\ell}_2 \gamma^\mu \ell_2 + X_{e_n} \bar{e}_n \gamma^\mu e_n + X_{\nu_n} \bar{\nu}_n \gamma^\mu \nu_n), \quad (2.12)$$

where $\Lambda_{ij}^{dL} := V_{dL}^\dagger \text{diag}(0, 0, 1) V_{dL}$.

3 SMEFT matching

Integrating out the heavy X boson and matching onto the SM Effective Field Theory (SMEFT) at a scale $M_X := g_X X_\theta v_X$, we obtain the Wilson coefficients (WCs) for dimension-6 SMEFT operators written in Table 3. The WCs $\{C_i\}$ have units of $[\text{mass}]^{-2}$ and are written in the Warsaw basis [76], a basis of a set of independent baryon-number conserving operators. By performing the matching between our models and the SMEFT, we obtain the set of WCs $\{C_i\}$ at the scale M_X , which can then be used to calculate predictions for observables.

Table 3 Non-zero dimension-6 SMEFT Wilson coefficients in the Warsaw basis, obtained by integrating out the heavy X boson at scale M_X .

WC	Value	WC	Value
C_{ll}^{2222}	$-\frac{1}{2} X_{\ell_2}^2$	$(C_{lq}^{(1)})^{22ij}$	$-X_{q3} X_{\ell_2} \Lambda_{ij}^{dL}$
$(C_{qq}^{(1)})^{ijkl}$	$X_{q3}^2 \Lambda_{ij}^{dL} \Lambda_{kl}^{dL} \frac{\delta_{ik} \delta_{jl} - 2}{2}$	C_{nnnn}^{nnnn}	$-\frac{1}{2} X_{e_n}^2$
C_{uu}^{3333}	$-\frac{1}{2} X_{u_3}^2$	C_{dd}^{3333}	$-\frac{1}{2} X_{d_3}^2$
C_{eu}^{nn33}	$-X_{e_n} X_{u_3}$	C_{ed}^{nn33}	$-X_{e_3} X_{d_3}$
$(C_{ud}^{(1)})^{3333}$	$-X_{u_3} X_{d_3}$	C_{le}^{22nn}	$-X_{\ell_2} X_{e_n}$
C_{lu}^{2233}	$-X_{\ell_2} X_{u_3}$	C_{ld}^{2233}	$-X_{\ell_2} X_{d_3}$
C_{qe}^{ijnn}	$-X_{q3} X_{e_n} \Lambda_{ij}^{dL}$	$(C_{qu}^{(1)})^{ij33}$	$-X_{q3} X_{u_3} \Lambda_{ij}^{dL}$
$(C_{qd}^{(1)})^{ij33}$	$-X_{q3} X_{d_3} \Lambda_{ij}^{dL}$	$(C_{\phi l}^{(1)})^{22}$	$-X_H X_{\ell_2}$
$(C_{\phi q}^{(1)})^{ij}$	$-X_H X_{q3}$	$C_{\phi e}^{nn}$	$-X_H X_{e_n}$
$C_{\phi u}^{33}$	$-X_H X_{u_3}$	$C_{\phi d}^{33}$	$-X_H X_{d_3}$
$C_{\phi D}$	$-2X_H^2$	$C_{\phi \square}$	$-\frac{1}{2} X_H^2$

We write the coefficients as functions of the charges X_f , which are explicitly parameterised in (2.5). The integer $n = 2$ or $n = 3$ corresponds to two variations of the model, as explained in Sect. 2. All Wilson coefficients are in units of g_X^2/M_X^2 .

4 Phenomenology

Starting from the SMEFT matching of Sect. 3, we will use the `smelli2.3.2` program to evaluate the likelihood of the model given hundreds of observables in the electroweak and flavour sectors. Before we do so, however, we think it important to highlight the most important observables that are sensitive to our model, and how these depend upon the SMEFT coefficients and hence upon the X_f charges.

4.1 Important observables

Electroweak

In light of the recent CDF II measurement [2], the M_W prediction is deserving of special attention. We can parameterise its deviation from the SM prediction in our Z' model via the parameter

$$\rho_0 := \frac{M_W^2}{M_Z^2 \hat{c}_Z^2 \hat{\rho}}, \quad (4.1)$$

where the parameter $\hat{\rho} = 1.01019 \pm 0.00009$ includes the custodial-violating top contributions to the gauge boson masses (see Ref. [75]). In (4.1), we use the conventional notation $\hat{c}_Z^2 := \cos^2 \hat{\theta}_w(M_Z) = \frac{\hat{g}^2(M_Z)}{\hat{g}^2(M_Z) + \hat{g}'^2(M_Z)}$ to denote the cosine squared of the renormalised Weinberg angle in the $\overline{\text{MS}}$ scheme. The ρ_0 parameter is defined so as to equal precisely 1 in the SM using the $\overline{\text{MS}}$ scheme. Its deviation from unity in our heavy Z' model, which recall is due to

$Z - Z'$ mixing, is

$$\rho_0 \approx 1 + \frac{4X_H^2 g_X^2}{g^2 + g'^2} \frac{M_Z^2}{M_{Z'}^2}. \quad (4.2)$$

Importantly, ρ_0 unavoidably shifts *upwards* [1,77], easing the tension due to the CDF II M_W measurement irrespective of the sign of the Higgs charge X_H .

At the level of the SMEFT, this shift is captured by the Wilson coefficients $C_{\phi D}$ and $C_{\phi\Box}$, which are (as in Table 3)

$$C_{\phi D} = 4C_{\phi\Box} = -2X_H^2 \frac{g_X^2}{M_X^2} = -18s^2 \frac{g_X^2}{M_X^2}. \quad (4.3)$$

Global fits of the SMEFT to electroweak data that turn on only these two operators have been found to give a good fit to electroweak data in light of the CDF measurement (e.g. [78]).

The status of the electroweak fit is of course much more delicate in our model for the $b \rightarrow s\ell\ell$ anomalies, because we have a plethora of new physics effects in Z pole observables due to modified Z couplings to fermions. Important among these are modified Z couplings to leptons, especially muons, and the forward-backward asymmetry variable A_b^{FB} for Z decays to $b\bar{b}$, because these observables already exhibit small tensions with the SM and because they receive large-ish corrections in our model. These effects are strictly correlated to the shifts in $C_{\phi D}$ and $C_{\phi\Box}$, since they arise from the $Z - Z'$ mixing.

$b \rightarrow s\ell\ell$

Regarding the $b \rightarrow s\ell\ell$ anomalies and related observables, the new physics effects can be parameterised by contributions to Wilson coefficients in the weak effective theory (WET). The WET Hamiltonian is, using a conventional normalisation,

$$\mathcal{H}_{\text{EFT}} = -\frac{4G_F}{\sqrt{2}} V_{tb} V_{ts}^* \sum_i (C_i^{\text{SM}} + C_i) \mathcal{O}_i, \quad (4.4)$$

where we emphasise that in the present paper, C_i denotes the *beyond* the SM (BSM) contribution to the Wilson coefficient. When coupling to $\bar{b}s/\bar{s}b$ currents, the Z' only couples to the left-handed component and so there are contributions to the dimension-6 semi-leptonic operators

$$\begin{aligned} \mathcal{O}_9^{\ell\ell} &= \frac{e^2}{16\pi^2} (\bar{s}\gamma_\mu P_L b) (\bar{\ell}\gamma^\mu \ell), \quad \ell \in \{e, \mu\}, \\ \mathcal{O}_{10}^{\ell\ell} &= \frac{e^2}{16\pi^2} (\bar{s}\gamma_\mu P_L b) (\bar{\ell}\gamma^\mu \gamma_5 \ell). \end{aligned} \quad (4.5)$$

Because of the $Z - Z'$ mixing, the Z boson picks up a small quark flavour-violating coupling to $\bar{b}s$, *viz.* $\mathcal{L} \supset$

$g_Z^{sb} Z_\mu \bar{b}_L \gamma^\mu s_L + H.c.$, where the coupling g_Z^{sb} is proportional to the $Z - Z'$ mixing angle (2.9). Specifically,

$$g_Z^{sb} = X_{q3} X_H \sin 2\theta_{sb} \frac{g_X^2}{g/c_w} \frac{M_Z^2}{M_{Z'}^2}. \quad (4.6)$$

There are thus BSM contributions to the 4-fermion operators $\mathcal{O}_{9,10}^{\ell\ell}$ from both Z exchange and from Z' exchange, and these are of the same order. The Z contributions are lepton flavour universal (LFU), whereas the Z' contributions introduce lepton flavour universality violation (LFUV).

Accounting for both contributions⁸ we have

$$\begin{aligned} C_9^{\mu\mu} &= -N(X_{\ell_2} + X_{e_2}) + C_9^U, \quad \text{where } C_9^U = NX_H/k \approx 0, \\ C_{10}^{\mu\mu} &= -N(-X_{\ell_2} + X_{e_2}) + C_{10}^U, \quad \text{where } C_{10}^U = -NX_H, \\ C_9^{ee} &= C_9^U \approx 0, \\ C_{10}^{ee} &= C_{10}^U, \end{aligned} \quad (4.8)$$

where recall that $k = 1/(1 - 4\sin^2 \theta_w) \approx 9.23$. We have defined the common pre-factor

$$N = \frac{\sqrt{2}\pi^2 \sin 2\theta_{sb} g_X^2 X_{q3}}{e^2 G_F V_{tb} V_{ts}^* M_{Z'}^2}, \quad (4.9)$$

where e is the electromagnetic gauge coupling. The Z -induced LFU pieces in (4.8) clearly vanish in the limit $X_H \rightarrow 0$, in which there is no $Z - Z'$ mixing. The LFU contributions to the $b \rightarrow s\ell\ell$ observables are therefore correlated to their effects on EWPOs, including the shift in M_W . This correlation was explored, prior to the updated CDF II measurement, in Ref. [77].

Substituting in the parametrisation (2.2–2.5) of charges in our models, and dropping the $1/k$ suppressed C_9^U contributions, we have

$$\begin{aligned} n = 3 : \quad C_9^{\mu\mu} &\approx 3N(-s - t), \\ C_{10}^{\mu\mu} &= 3N(2s + t), \\ C_{10}^{ee} &= 3Ns. \end{aligned} \quad (4.10)$$

This is equivalent to writing the chirality of the coupling to muons in terms of left and right projection operators as in

⁸ Of course these contributions to the WET coefficients can also be derived at the level of the SMEFT matching. From this perspective, the SMEFT-WET matching formulae are [79,80]:

$$\begin{aligned} C_9^{ij} &= \frac{4\pi^2}{e^2} \frac{v^2}{V_{tb} V_{ts}^*} \left[-\frac{1}{k} \left(C_{\phi q}^{(1)23} + C_{\phi q}^{(3)23} \right) + C_{\ell q}^{(1)ij23} + C_{\ell q}^{(3)ij23} + C_{qe}^{23ij} \right] \\ C_{10}^{ij} &= \frac{4\pi^2}{e^2} \frac{v^2}{V_{tb} V_{ts}^*} \left[C_{\phi q}^{(1)23} + C_{\phi q}^{(3)23} - C_{\ell q}^{(1)ij23} - C_{\ell q}^{(3)ij23} + C_{qe}^{23ij} \right]. \end{aligned} \quad (4.7)$$

Substituting in the SMEFT Wilson coefficients from Table 3 reproduces (4.8).

Sect. 1, i.e. via an effective operator $\propto (\bar{s}\gamma_\mu P_L b)(\bar{\mu}\gamma^\mu P_X \mu)$. For a general s and t , this projection operator is

$$P_X = P_L - \frac{s}{3s + 2t} P_R \quad (n = 3). \quad (4.11)$$

For the variation of the model with $n = 2$, we have

$$\begin{aligned} n = 2 : \quad C_9^{\mu\mu} &\approx 3N(-3s - 2t), \\ C_{10}^{\mu\mu} &= 0, \\ C_{10}^{ee} &= 3Ns, \end{aligned} \quad (4.12)$$

thus $P_X \approx P_L + P_R$, a vectorial coupling of the Z' to $\mu^+ \mu^-$.

4.2 Global fits

We wrote a computer program (included in the ancillary information attached to the arXiv preprint of this paper) that uses `smelli2.3.2` to calculate the likelihoods of 277 observables for our model by first calculating the WCs in Table 3 at scale M_X . `smelli2.3.2` then renormalises the SMEFT operators down to the scale M_Z , where it calculates the EWPOs. It then matches at tree-level to the weak effective theory, and renormalises the resulting WCs down to the scale of the mass of the bottom quark, where the various observables pertinent to B -meson decays are calculated.

For a given s and t the likelihoods are a function of two effective parameters: $\alpha := g_X \times 3 \text{ TeV}/M_X$ and the quark mixing angle θ_{sb} . Throughout, we shall illustrate with $M_X = 3 \text{ TeV}$ as an example (similar third-family type models with $M_X \geq 1 \text{ TeV}$ were not ruled out by search constraints in the parameter region where they fit the $b \rightarrow s\ell\ell$ anomalies [81,82] and so we expect $M_X = 3 \text{ TeV}$ to be allowed by direct Z' search constraints). We do not expect a significant change if we were to change M_X to a different value $M_{X'}$ as long as one scales g_X by the same factor, since the boundary conditions upon the Wilson coefficients (shown in Table 3) depend only upon the ratio g_X/M_X . This approximation is good up to small loop suppressed corrections from the renormalisation group running between $M_{X'}$ and M_X , which induce relative multiplicative changes of $\mathcal{O}[\log(M_{X'}/M_X)/(16\pi^2)]$ in corrections to predictions of observables⁹.

We consider each different value of the ratio t/s to constitute a different model. `smelli2.3.2` then calculates χ^2 via the predicted values of observables. We minimise χ^2 by varying α and θ_{sb} using the Nelder–Mead algorithm, given a guess at a starting point. This was obtained by doing a rough initial scan for one value of $t \neq 0$ and $s \neq 0$ and roughly estimating how electroweak and b -observable χ^2 values are expected to scale with s and t .

⁹ Strictly speaking, we calculated the fit at a reference point of $M_X = 1 \text{ TeV}$.

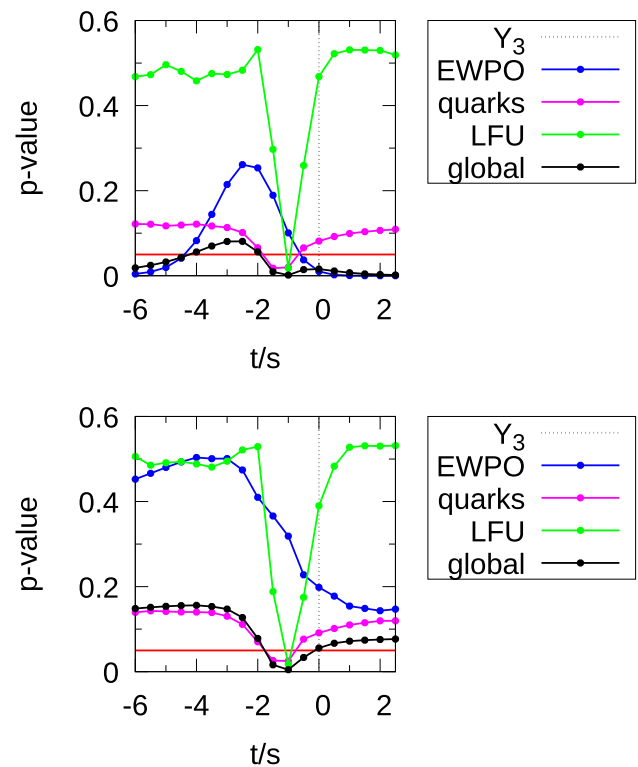


Fig. 1 p values for different models depending upon t/s , for $n = 3$. The top panel includes the recent CDF measurement of M_W as in (1.1), whereas in the bottom panel, the default `smelli2.3.2` constraint (i.e. excluding the recent CDF measurement) on M_W was used as in (4.13). The Third Family Hypercharge Model is marked in the legend by Y_3 . Only the global p value accounts for the 2 fitted parameters in the calculation of the number of degrees of freedom. We consider global p values above the red line at 0.05 to be acceptable fits to the data

The result, for a given value of t/s , is a best-fit point, where the fit in the EWPOs is balanced against those of the b data. This balance crucially depends upon the experimental constraint that is taken on M_W , as we illustrate in the top panel of Fig. 1, where we display p values using (1.1), which includes the CDF II measurement. Here, we can see that, for example, the Third Family Hypercharge Model model, denoted Y_3 , is somewhat disfavoured: its global p value is around .02. Models at larger values of $|t/s|$ approximate the $B_3 - L_3$ model and so the p values all asymptote towards the left-hand side and the right-hand side of the plot. The $B_3 - L_3$ model has no $Z - Z'$ mixing because the Higgs doublet field is not charged under $B_3 - L_3$, meaning that in the limit of large $|t/s|$, the CDF II M_W measurement strongly disfavours each model. We see that models with $-5 < t/s < -2$ all fare well with global p values above the canonical .05 bound shown by the red line. We notice by examining the EWPO p values that the M_W constraint prefers a localised value of t/s . The other effects that are relevant are in the LFU and ‘quarks’ categories: both have a valley around $t/s = -1$. Here, at $s = -t$, one can see from (2.2) that $X_{q_3} = X_{\ell_2} = 0$, meaning

that there is no coupling at tree-level between the Z' and left-handed quarks or left-handed muons; the Z' does therefore not help with the $b \rightarrow s\ell\ell$ anomalies and we revert to the poor fit of the SM both for the ‘LFU’ and for the ‘quarks’ category of observable. It is of interest that the p value is suppressed somewhat for all t/s by the ‘quarks’ category of observable, in which there is room for disagreement with the theoretical uncertainty budget of the prediction.

We see a rather weak M_W selection effect in the bottom panel of Fig. 1 for the default experimental M_W constraint in `smelli2.3.2`, which amounts to

$$M_W = 80.3795 \pm 0.0121 \text{ GeV} \quad (4.13)$$

(the central value of the SM prediction according to `smelli2.3.2` is $M_W = 80.3509 \text{ GeV}$). The `smelli2.3.2` M_W constraint leads to weaker selection than the one including the CDF II M_W measurement because it has much larger uncertainties and less need for a large contribution from the Z' . We see here that only the region $-2 < t/s < 0$ has a global p value of *less* than .05, and this is clearly driven by the ‘quarks’ and ‘LFU’ categories, not by EWPOs. We summarise the χ^2 and p values for both options of experimental M_W constraint in Table 4.

We now go on to examine the pulls at each best-fit point for $t/s = -3$. We define the pull for an observable with theoretical prediction P , measured central value M and uncertainty C to be

$$\text{pull} = \frac{P - M}{C}, \quad (4.14)$$

where C does *not* include correlations with other observables, but may include theoretical uncertainties added in quadrature in some cases. In particular, for M_W , we have added an estimated uncertainty in the prediction of 5.6 MeV [4] in quadrature.

We display the pulls for the combination of M_W measurements that include the recent CDF II determination in Fig. 2. Several notable effects are evident: for example, unsurprisingly M_W itself is better fit, with a pull of -1 . The observable R_μ , the branching ratio of the Z^0 boson to $\mu^+\mu^-$, has been increased by a fair amount; in the SM the prediction was high by over 1σ , but in the Z' model with $t/s = -3$ it is less than one sigma too low¹⁰. We see that the forward-backward asymmetry measured in $e^+e^- \rightarrow b\bar{b}$, A_{FB}^b , has a worse fit in the Z' model. A_e , the left-right asymmetry in $e^+e^- \rightarrow e^+e^-$, has a smaller pull in the Z' model. Overall, the quality of fit to

the EWPOs is fine: Table 4 shows that the p -value is .29. The right-hand panel of Fig. 2 shows that many of the selected observables of interest to b -meson decays are fit better than in the SM save for the $B_s - \bar{B}_s$ mixing observable Δm_s , which receives (fairly mild) positive corrections from the Z' contribution.

We compare and contrast the fits *including* the CDF II M_W measurement from Fig. 2 with fits *excluding* it in Fig. 3. The most obvious effect of excluding the CDF II M_W measurement is that the SM pull of M_W of is only 2σ when the CDF II M_W measurement is excluded. Because the required shift in M_W is smaller, the relative effect upon the other EWPOs is smaller and the result is a good fit to EWPOs for $t/s = -3$: Table 4 reveals the p value in the fit to be .49. The fits in the b -observables on the right-hand panel show a very similar pattern between Figs. 2 and 3. Essentially, g_X is being fixed by the EWPOs (and is being pulled by M_W in particular), and then θ_{sb} is fit to a value which fits the $b \rightarrow s\ell\ell$ anomalies. Here, many of the SM-discrepant observables relevant to the b -anomalies receive a relative contribution from the Z' [50] $\propto g_X^2 \sin 2\theta_{sb}/M_X^2$. We see that the pull of Δm_s , which is a measure of the $B_s - \bar{B}_s$ mixing, decreases when one includes the CDF II M_W measurement. This is because the fit is pushed to a larger value of g_X in order to fit the larger needed new physics contribution in M_W . In turn, in order to fit the b -anomalies, one requires a smaller value of θ_{sb} in order to keep the Z' contributions to them (4.9) constant, in turn reducing the Z' contribution to $B_s - \bar{B}_s$ mixing.

The p values and pulls for the $n = 2$ fits are qualitatively similar to those for $n = 3$ and we neglect to present them here, noting that they are presented in the ancillary information attached to the arXiv preprint version of this paper. Excluding all of the M_W measurements except for the CDF II one, the fits do not differ in significant details (the global p values differ by less than .02, for example) and we also relegate plots for them to the ancillary information.

5 Conclusions

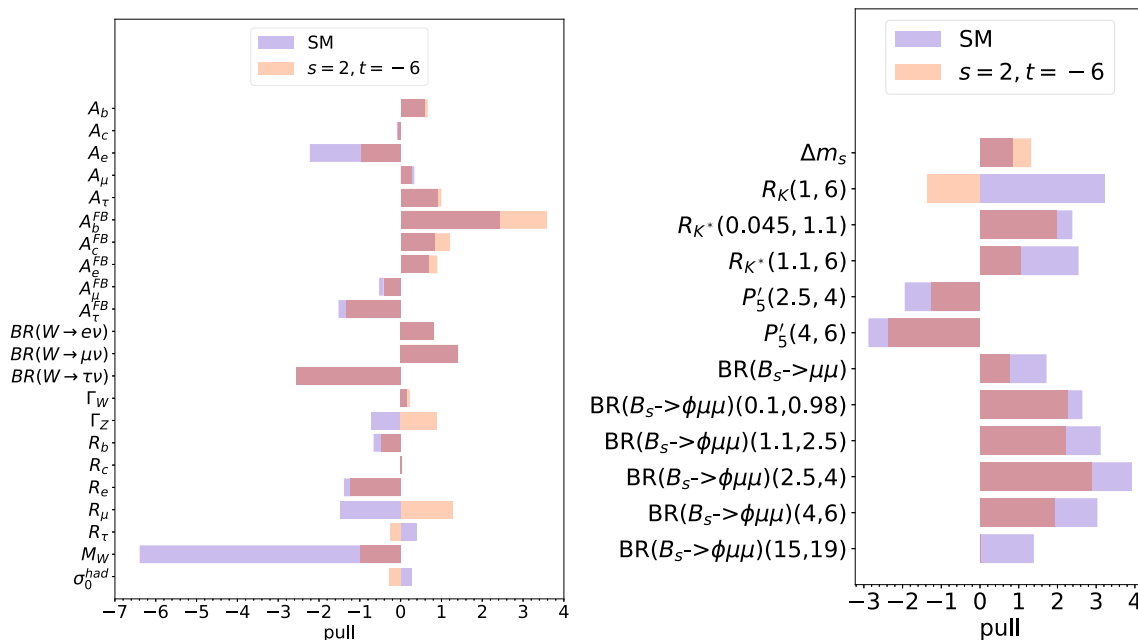
A Z' model where the SM is augmented by an additional, spontaneously broken $U(1)$ gauge group can simultaneously fit both the CDF M_W anomaly and the $b \rightarrow s\ell\ell$ anomalies. The model retains the other desirable properties of the Y_3 model on which it is based [50]: namely that it qualitatively explains a hierarchically heavy third generation of quarks and small CKM angles. As Fig. 1 demonstrates, the log likelihood contribution from CDF’s M_W measurement is instrumental in picking out favoured values for the $U(1)_X$ quantum numbers of the fields. A particularly simple anomaly-free combination $Y_3 - 3(B_3 - L_3)$ has a high quality of fit (where the ℓ_3 field is subsequently identified with the left-handed *muon* lepton

¹⁰ Observables such as R_μ receive contributions from $(C_{\phi l}^{(1)})^{22}$, $C_{\phi e}^{22}$. As a reference to Table 3 and (2.2–2.5) shows, the sign of these contributions depends upon the sign of t/s . We have checked that the predictions for such observables do indeed go in the ‘wrong’ direction for positive t/s , resulting in a less favourable fit.

Table 4 p values for $s = 2, t = -6$ for the two different constraints upon M_W and $n = 3$.

Category	χ^2	n_{obs}	p value
Including CDF II M_W (1.1)			
$g_X \times 3 \text{ TeV}/M_{Z'} = 0.0209, \theta_{sb} = -0.0191$			
Quarks	246.7	224	.11
LFU FCNCs	22.8	23	.47
EWPOs	35.8	30	.21
Global	305.3	277	.08
Default <code>smelli2.3.2</code> M_W (4.13)			
$g_X \times 3 \text{ TeV}/M_{Z'} = 0.0150, \theta_{sb} = -0.0361$			
Quarks	248.7	224	.13
LFU FCNCs	22.4	23	.50
EWPOs	30.3	31	.49
Global	301.4	278	.14

The default `smelli2.3.2` M_W experimental constraint includes two input experimental values: one from ATLAS [83] and one combined measurement from CDF plus Dzero [84], whereas we use a single combined value from Ref. [4] when we include the CDF II constraint upon M_W . This fact explains why $n_{obs}(\text{EWPOs})$ differs by 1 between the two different M_W constraint options. We also display the best-fit model parameters for each option of experimental M_W constraint

**Fig. 2** Pulls of interest including the recent CDF measurement of M_W i.e. (1.1) and $n = 3$. In the left-hand panel, we display the EWPOs, whereas in the right-hand panel, we display selected observables of interest to $b \rightarrow sl^+l^-$ anomalies

doublet¹¹). We note that for the combination $Y_3 - 3(B_3 - L_3)$, the ‘LFU’ and ‘EWPO’ classes of observable (both of which have small theoretical uncertainties) each separately have a better quality of fit than the ‘quarks’ class, where there is more room for argument about the prediction and the size of the theoretical uncertainty assigned.

¹¹ Identifying e_3 with the right-handed muon field in addition also provides a similarly acceptable fit.

We have not developed details of the ultra-violet model, preferring instead to begin by working with an effective theory with $SU(3) \times SU(2)_L \times U(1)_Y \times U(1)_X$ gauge symmetry¹². Light family Yukawa couplings are expected to result from some non-renormalisable operators, having integrated out heavy multi-TeV fermions that are vector-like represen-

¹² The sub-Planckian Landau poles [85] in g_X may then be mitigated by new heavy (but sub-Planckian) states originating from a larger non-abelian symmetry that is spontaneously broken to $SM \times U(1)_X$.

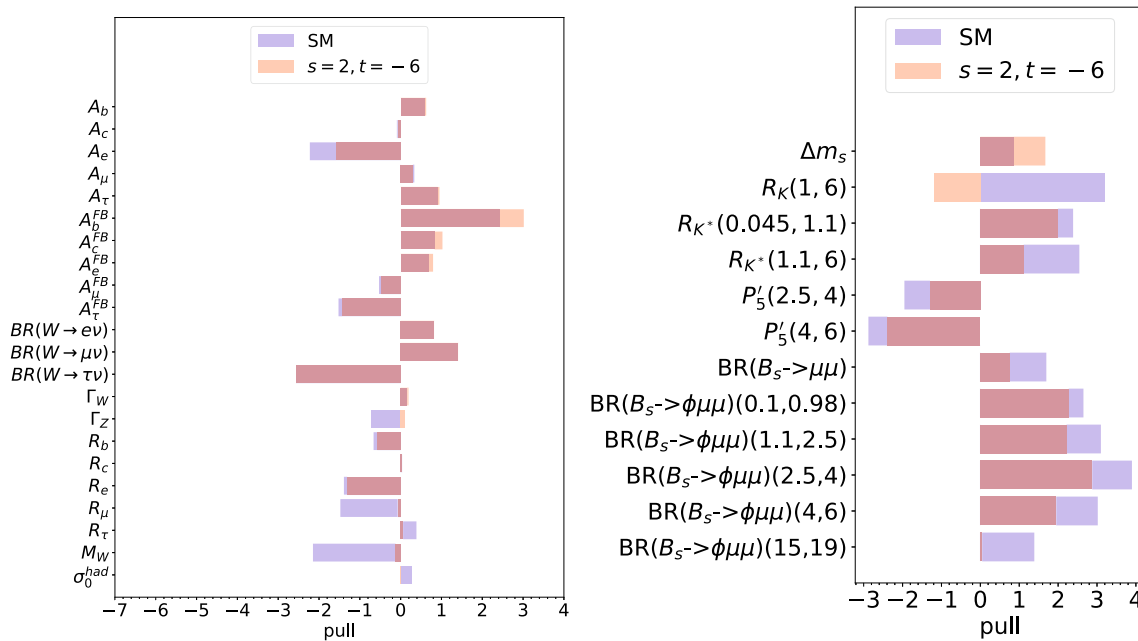


Fig. 3 Pulls of interest for the default $smelli2.3.2$ constraint on M_W (i.e. excluding the recent CDF measurement) and $n = 3$ as in (4.13). In the left-hand panel, we display the EWPOs, whereas in the right-hand panel, we display selected observables of interest to $b \rightarrow sl+l^-$ anomalies

tations of the gauge group, for example. We argue, following Ref. [86], that it is premature to set the details of the model in the ultra-violet more than we have, preferring instead to allow the data (such as the new measurement of M_W) to inform the model building in a more fundamental and vital way. Indeed, we have used it in the present paper to select $U(1)_X$ charges under the symmetry group.

In the coming years, the LHC experiments will provide valuable further empirical measurements of M_W and observables pertinent to the $b \rightarrow sl\ell$ anomalies and Belle II data will also weigh in. In the meantime, an obvious avenue of interest is from direct searches for the Z' . The most promising channels [81] are likely to be $pp \rightarrow Z' \rightarrow \mu^+\mu^-$ with or without additional b -jets. LHC and HL-LHC sensitivity estimates are an obvious target for our models for future study.¹³

Acknowledgements This work has been partly supported by STFC HEP Theory Consolidated Grant ST/T000694/1. BCA thanks other members of the Cambridge Pheno Working Group for useful discussions. JD is supported by the SNF under contract 200020-204428, and by the European Research Council (ERC) under the European Union's Horizon 2020 research and innovation programme, Grant Agreement 833280 (FLAY). We thank P Stangl for helpful communications about $smelli2.3.2$ and A Crivellin for useful comments on the manuscript. We further thank G Hiller, D Litim, T Steudtner, and especially T H  hne for enlightening discussions.

¹³ Re-casts of LHC Run II Z' searches for similar models (e.g. the Y_3 and $B_3 - L_3$ models) indicate that the bounds are currently rather weak [81].

Data Availability Statement This manuscript has no associated data or the data will not be deposited. [Authors' comment: This is a theoretical study and no experimental data has been listed.]

Open Access This article is licensed under a Creative Commons Attribution 4.0 International License, which permits use, sharing, adaptation, distribution and reproduction in any medium or format, as long as you give appropriate credit to the original author(s) and the source, provide a link to the Creative Commons licence, and indicate if changes were made. The images or other third party material in this article are included in the article's Creative Commons licence, unless indicated otherwise in a credit line to the material. If material is not included in the article's Creative Commons licence and your intended use is not permitted by statutory regulation or exceeds the permitted use, you will need to obtain permission directly from the copyright holder. To view a copy of this licence, visit <http://creativecommons.org/licenses/by/4.0/>.

Funded by SCOAP³. SCOAP³ supports the goals of the International Year of Basic Sciences for Sustainable Development.

References

1. B.C. Allanach, J.E. Camargo-Molina, J. Davighi, Global fits of third family hypercharge models to neutral current B-anomalies and electroweak precision observables. [arXiv:2103.12056](https://arxiv.org/abs/2103.12056)
2. CDF collaboration, High-precision measurement of the W boson mass with the CDF II detector. *Science* **376**, 170 (2022)
3. C.-T. Lu, L. Wu, Y. Wu, B. Zhu, Electroweak precision fit and new physics in light of W boson mass. [arXiv:2204.03796](https://arxiv.org/abs/2204.03796)
4. J. de Blas, M. Pierini, L. Reina, L. Silvestrini, Impact of the recent measurements of the top-quark and W-boson masses on electroweak precision fits. [arXiv:2204.04204](https://arxiv.org/abs/2204.04204)
5. J. Aebischer, J. Kumar, P. Stangl, D.M. Straub, A global likelihood for precision constraints and flavour anomalies. *Eur. Phys. J. C* **79**, 509 (2019). [[arXiv:1810.07698](https://arxiv.org/abs/1810.07698)]

6. LHCb collaboration, Test of lepton universality with $B^0 \rightarrow K^{*0} \ell^+ \ell^-$ decays. JHEP **08**, 055 (2017). [arXiv:1705.05802](#)
7. LHCb collaboration, Search for lepton-universality violation in $B^+ \rightarrow K^+ \ell^+ \ell^-$ decays. Phys. Rev. Lett. **122**, 191801 (2019). [arXiv:1903.09252](#)
8. LHCb collaboration, Test of lepton universality in beauty-quark decays. Nat. Phys. **18**, 277 (2022). [arXiv:2103.11769](#)
9. LHCb collaboration, Tests of lepton universality using $B^0 \rightarrow K_S^{*0} \ell^+ \ell^-$ and $B^+ \rightarrow K^{*+} \ell^+ \ell^-$ decays. Phys. Rev. Lett. **128**, 191802 (2022). [arXiv:2110.09501](#)
10. ATLAS collaboration, Study of the rare decays of B_s^0 and B^0 mesons into muon pairs using data collected during 2015 and 2016 with the ATLAS detector. JHEP **04**, 098 (2019). [arXiv:1812.03017](#)
11. CMS collaboration, Measurement of the $B_s^0 \rightarrow \mu^+ \mu^-$ branching fraction and search for $B^0 \rightarrow \mu^+ \mu^-$ with the CMS experiment. Phys. Rev. Lett. **111**, 101804 (2013). [arXiv:1307.5025](#)
12. CMS, LHCb collaboration, Observation of the rare $B_s^0 \rightarrow \mu^+ \mu^-$ decay from the combined analysis of CMS and LHCb data. Nature **522**, 68 (2015). [arXiv:1411.4413](#)
13. LHCb collaboration, Measurement of the $B_s^0 \rightarrow \mu^+ \mu^-$ branching fraction and effective lifetime and search for $B^0 \rightarrow \mu^+ \mu^-$ decays. Phys. Rev. Lett. **118**, 191801 (2017). [arXiv:1703.05747](#)
14. LHCb collaboration, Analysis of neutral B-meson decays into two muons. Phys. Rev. Lett. **128**, 041801 (2022). [arXiv:2108.09284](#)
15. LHCb collaboration, Measurement of form-factor-independent observables in the decay $B^0 \rightarrow K^{*0} \mu^+ \mu^-$. Phys. Rev. Lett. **111**, 191801 (2013). [arXiv:1308.1707](#)
16. LHCb collaboration, Angular analysis of the $B^0 \rightarrow K^{*0} \mu^+ \mu^-$ decay using 3 fb^{-1} of integrated luminosity. JHEP **02**, 104 (2016). [arXiv:1512.04442](#)
17. ATLAS collaboration, Angular analysis of $B_d^0 \rightarrow K^{*0} \mu^+ \mu^-$ decays in pp collisions at $\sqrt{s} = 8 \text{ TeV}$ with the ATLAS detector. JHEP **10**, 047 (2018). [arXiv:1805.04000](#)
18. CMS collaboration, Measurement of angular parameters from the decay $B^0 \rightarrow K^{*0} \mu^+ \mu^-$ in proton-proton collisions at $\sqrt{s} = 8 \text{ TeV}$. Phys. Lett. B **781**, 517 (2018). [arXiv:1710.02846](#)
19. CMS collaboration, Angular analysis of the decay $B^0 \rightarrow K^{*0} \mu^+ \mu^-$ from pp collisions at $\sqrt{s} = 8 \text{ TeV}$. Phys. Lett. B **753**, 424 (2016). [arXiv:1507.08126](#)
20. C. Bobeth, M. Chrzaszcz, D. van Dyk, J. Virto, Long-distance effects in $B \rightarrow K^{*} \ell \ell$ from analyticity. Eur. Phys. J. C **78**, 451 (2018). [arXiv:1707.07305](#)
21. LHCb collaboration, Angular analysis and differential branching fraction of the decay $B_s^0 \rightarrow \phi \mu^+ \mu^-$. JHEP **09**, 179 (2015). [arXiv:1506.08777](#)
22. CDF collaboration, Precise measurements of exclusive $b \rightarrow s \mu^+ \mu^-$ -decay amplitudes using the full CDF data set
23. M. Algueró, B. Capdevila, A. Crivellin, S. Descotes-Genon, P. Masjuan, J. Matias et al., Emerging patterns of new physics with and without lepton flavour universal contributions. Eur. Phys. J. C **79**, 714 (2019). [arXiv:1903.09578](#)
24. A.K. Alok, A. Dighe, S. Gangal, D. Kumar, Continuing search for new physics in $b \rightarrow s \mu \mu$ decays: two operators at a time. JHEP **06**, 089 (2019). [arXiv:1903.09617](#)
25. M. Ciuchini, A.M. Coutinho, M. Fedele, E. Franco, A. Paul, L. Silvestrini et al., New Physics in $b \rightarrow s \ell^+ \ell^-$ confronts new data on Lepton Universality. Eur. Phys. J. C **79**, 719 (2019). [arXiv:1903.09632](#)
26. J. Aebischer, W. Altmannshofer, D. Guadagnoli, M. Reboud, P. Stangl, D.M. Straub, B -decay discrepancies after Moriond 2019. Eur. Phys. J. C **80**, 252 (2020). [arXiv:1903.10434](#)
27. A. Datta, J. Kumar, D. London, The B anomalies and new physics in $b \rightarrow s e^+ e^-$. Phys. Lett. B **797**, 134858 (2019). [arXiv:1903.10086](#)
28. K. Kowalska, D. Kumar, E.M. Sessolo, Implications for new physics in $b \rightarrow s \mu \mu$ transitions after recent measurements by Belle and LHCb. Eur. Phys. J. C **79**, 840 (2019). [arXiv:1903.10932](#)
29. A. Arbey, T. Hurth, F. Mahmoudi, D.M. Santos, S. Neshatpour, Update on the $b \rightarrow s$ anomalies. Phys. Rev. D **100**, 015045 (2019). [arXiv:1904.08399](#)
30. U. Egede, S. Nishida, M. Patel, M.-H. Schune, Electroweak penguin decays of b -flavoured hadrons. [arXiv:2205.05222](#)
31. W. Altmannshofer, P. Stangl, New physics in rare B decays after Moriond 2021. [arXiv:2103.13370](#)
32. R. Gauld, F. Goertz, U. Haisch, On minimal Z' explanations of the $B \rightarrow K^{*} \mu^+ \mu^-$ anomaly. Phys. Rev. D **89**, 015005 (2014). [arXiv:1308.1959](#)
33. A.J. Buras, F. De Fazio, J. Girrbach, 331 models facing new $b \rightarrow s \mu^+ \mu^-$ data. JHEP **02**, 112 (2014). [arXiv:1311.6729](#)
34. A.J. Buras, J. Girrbach, Left-handed Z' and Z FCNC quark couplings facing new $b \rightarrow s \mu^+ \mu^-$ data. JHEP **12**, 009 (2013). [arXiv:1309.2466](#)
35. A.J. Buras, F. De Fazio, J. Girrbach-Noe, Z - Z' mixing and Z -mediated FCNCs in $SU(3)_C \times SU(3)_L \times U(1)_X$ models. JHEP **08**, 039 (2014). [arXiv:1405.3850](#)
36. B. Allanach, F.S. Queiroz, A. Strumia, S. Sun, Z' models for the LHCb and $g-2$ muon anomalies. Phys. Rev. D **93**, 055045 (2016). [arXiv:1511.07447](#)
37. B. Allanach, B. Gripaios, J. Tooby-Smith, Anomaly cancellation with an extra gauge boson. [arXiv:2006.03588](#)
38. B.C. Allanach, J. Davighi, S. Melville, An anomaly-free Atlas: charting the space of flavour-dependent gauged $U(1)$ extensions of the Standard Model. JHEP **02**, 082 (2019). [arXiv:1812.04602](#)
39. J. Davighi, B. Gripaios, N. Lohitsiri, Global anomalies in the Standard Model(s) and beyond. JHEP **07**, 232 (2020). [arXiv:1910.11277](#)
40. E. Witten, An $SU(2)$ anomaly. Phys. Lett. B **117**, 324 (1982)
41. W. Altmannshofer, S. Gori, M. Pospelov, I. Yavin, Quark flavor transitions in $L_\mu - L_\tau$ models. Phys. Rev. D **89**, 095033 (2014). [arXiv:1403.1269](#)
42. A. Crivellin, G. D'Ambrosio, J. Heeck, Explaining $h \rightarrow \mu^\pm \tau^\mp$, $B \rightarrow K^{*} \mu^+ \mu^-$ and $B \rightarrow K \mu^+ \mu^- / B \rightarrow K e^+ e^-$ in a two-Higgs-doublet model with gauged $L_\mu - L_\tau$. Phys. Rev. Lett. **114**, 151801 (2015). [arXiv:1501.00993](#)
43. A. Crivellin, G. D'Ambrosio, J. Heeck, Addressing the LHC flavor anomalies with horizontal gauge symmetries. Phys. Rev. D **91**, 075006 (2015). [arXiv:1503.03477](#)
44. A. Crivellin, L. Hofer, J. Matias, U. Nierste, S. Pokorski, J. Rosiek, Lepton-flavour violating B decays in generic Z' models. Phys. Rev. D **92**, 054013 (2015). [arXiv:1504.07928](#)
45. W. Altmannshofer, I. Yavin, Predictions for lepton flavor universality violation in rare B decays in models with gauged $L_\mu - L_\tau$. Phys. Rev. D **92**, 075022 (2015). [arXiv:1508.07009](#)
46. J. Davighi, M. Kirk, M. Nardecchia, Anomalies and accidental symmetries: charging the scalar leptoquark under $L_\mu - L_\tau$. JHEP **12**, 111 (2020). [arXiv:2007.15016](#)
47. R. Alonso, P. Cox, C. Han, T. Yanagida, Flavoured $B - L$ local symmetry and anomalous rare B decays. Phys. Lett. B **774**, 643 (2017). [arXiv:1705.03858](#)
48. C. Bonilla, T. Modak, R. Srivastava, J.W.F. Valle, $U(1)_{B_3-3L_\mu}$ gauge symmetry as a simple description of $b \rightarrow s$ anomalies. Phys. Rev. D **98**, 095002 (2018). [arXiv:1705.00915](#)
49. B. Allanach, $U(1)_{B_3-L_2}$ explanation of the neutral current B -anomalies. [arXiv:2009.02197](#)
50. B. Allanach, J. Davighi, Third family hypercharge model for $R_{K^{(*)}}$ and aspects of the fermion mass problem. JHEP **12**, 075 (2018). [arXiv:1809.01158](#)
51. J. Davighi, Connecting neutral current B anomalies with the heaviness of the third family, in 54th Rencontres de Moriond on QCD and high energy interactions, ARISF, 5 (2019). [arXiv:1905.06073](#)
52. B. Allanach, J. Davighi, Naturalising the third family hypercharge model for neutral current B -anomalies. Eur. Phys. J. C **79**, 908 (2019). [arXiv:1905.10327](#)

53. D. Aristizabal Sierra, F. Staub, A. Vicente, Shedding light on the $b \rightarrow s$ anomalies with a dark sector. *Phys. Rev. D* **92**, 015001 (2015). [arXiv:1503.06077](#)
54. A. Celis, J. Fuentes-Martin, M. Jung, H. Serodio, Family nonuniversal Z' models with protected flavor-changing interactions. *Phys. Rev. D* **92**, 015007 (2015). [arXiv:1505.03079](#)
55. A. Greljo, G. Isidori, D. Marzocca, On the breaking of Lepton Flavor Universality in B decays. *JHEP* **07**, 142 (2015). [arXiv:1506.01705](#)
56. A. Falkowski, M. Nardecchia, R. Ziegler, Lepton flavor non-universality in B-meson decays from a $U(2)$ flavor model. *JHEP* **11**, 173 (2015). [arXiv:1509.01249](#)
57. C.-W. Chiang, X.-G. He, G. Valencia, Z' model for $b \rightarrow s\ell\bar{\ell}$ flavor anomalies. *Phys. Rev. D* **93**, 074003 (2016). [arXiv:1601.07328](#). <https://inspirehep.net/literature/1417096>
58. S.M. Boucenna, A. Celis, J. Fuentes-Martin, A. Vicente, J. Virto, Non-abelian gauge extensions for B-decay anomalies. *Phys. Lett. B* **760**, 214 (2016). [arXiv:1604.03088](#)
59. S.M. Boucenna, A. Celis, J. Fuentes-Martin, A. Vicente, J. Virto, Phenomenology of an $SU(2) \times SU(2) \times U(1)$ model with lepton flavour non-universality. *JHEP* **12**, 059 (2016). [arXiv:1608.01349](#)
60. P. Ko, Y. Omura, Y. Shigekami, C. Yu, LHCb anomaly and B physics in flavored Z' models with flavored Higgs doublets. *Phys. Rev. D* **95**, 115040 (2017). [arXiv:1702.08666](#)
61. R. Alonso, P. Cox, C. Han, T.T. Yanagida, Anomaly-free local horizontal symmetry and anomaly-free rare B-decays. *Phys. Rev. D* **96**, 071701 (2017). [arXiv:1704.08158](#)
62. Y. Tang, Y.-L. Wu, Flavor non-universal gauge interactions and anomalies in B-meson decays. *Chin. Phys. C* **42**, 033104 (2018). [arXiv:1705.05643](#)
63. D. Bhatia, S. Chakraborty, A. Dighe, Neutrino mixing and R_K anomaly in $U(1)_X$ models: a bottom-up approach. *JHEP* **03**, 117 (2017). [arXiv:1701.05825](#)
64. K. Fuyuto, H.-L. Li, J.-H. Yu, Implications of hidden gauged $U(1)$ model for B anomalies. *Phys. Rev. D* **97**, 115003 (2018). [arXiv:1712.06736](#)
65. L. Bian, H.M. Lee, C.B. Park, B-meson anomalies and Higgs physics in flavored $U(1)'$ model. *Eur. Phys. J. C* **78**, 306 (2018). [arXiv:1711.08930](#)
66. S.F. King, $R_{K^{(*)}}$ and the origin of Yukawa couplings. *JHEP* **09**, 069 (2018). [arXiv:1806.06780](#)
67. G.H. Duan, X. Fan, M. Frank, C. Han, J.M. Yang, A minimal $U(1)'$ extension of MSSM in light of the B decay anomaly. *Phys. Lett. B* **789**, 54 (2019). [arXiv:1808.04116](#)
68. Z. Kang, Y. Shigekami, $(g - 2)_\mu$ versus flavor changing neutral current induced by the light $(B - L)_{\mu\tau}$ boson. *JHEP* **11**, 049 (2019). [arXiv:1905.11018](#)
69. L. Calibbi, A. Crivellin, F. Kirk, C.A. Manzari, L. Vernazza, Z' models with less-minimal flavour violation. *Phys. Rev. D* **101**, 095003 (2020). [arXiv:1910.00014](#)
70. W. Altmannshofer, J. Davighi, M. Nardecchia, Gauging the accidental symmetries of the standard model, and implications for the flavor anomalies. *Phys. Rev. D* **101**, 015004 (2020). [arXiv:1909.02021](#)
71. B. Capdevila, A. Crivellin, C.A. Manzari, M. Montull, Explaining $b \rightarrow s\ell^+\ell^-$ and the Cabibbo angle anomaly with a vector triplet. *Phys. Rev. D* **103**, 015032 (2021). [arXiv:2005.13542](#)
72. J. Davighi, Anomalous Z' bosons for anomalous B decays. *JHEP* **08**, 101 (2021). [arXiv:2105.06918](#)
73. J. Davighi, Topological effects in particle physics phenomenology (2020). <https://doi.org/10.17863/CAM.47560>
74. J. Davighi, J. Tooby-Smith, Flatland: abelian extensions of the Standard Model with semi-simple completions. [arXiv:2206.11271](#)
75. Particle Data Group collaboration, Review of particle physics. *PTEP* **2020**, 083C01 (2020)
76. B. Grzadkowski, M. Iskrzynski, M. Misiak, J. Rosiek, Dimension-six terms in the Standard Model Lagrangian. *JHEP* **10**, 085 (2010). [arXiv:1008.4884](#)
77. M. Algueró, A. Crivellin, C.A. Manzari, J. Matias, Importance of $Z - Z'$ mixing in $b \rightarrow s\ell^+\ell^-$ and the W mass. [arXiv:2201.08170](#)
78. E. Bagnaschi, J. Ellis, M. Madigan, K. Mimasu, V. Sanz, T. You, SMEFT analysis of m_W . [arXiv:2204.05260](#)
79. J. Aebischer, A. Crivellin, M. Fael, C. Greub, Matching of gauge invariant dimension-six operators for $b \rightarrow s$ and $b \rightarrow c$ transitions. *JHEP* **05**, 037 (2016). [arXiv:1512.02830](#)
80. E.E. Jenkins, A.V. Manohar, P. Stoffer, Low-energy effective field theory below the electroweak scale: operators and matching. *JHEP* **03**, 016 (2018). [arXiv:1709.04486](#)
81. B.C. Allanach, H. Banks, Hide and seek with the third family hypercharge model's Z' at the large hadron collider. *Eur. Phys. J. C* **82**, 279 (2022). [arXiv:2111.06691](#)
82. B.C. Allanach, J.M. Butterworth, T. Corbett, Large hadron collider constraints on some simple Z' models for $b \rightarrow s\mu^+\mu^-$ anomalies. *Eur. Phys. J. C* **81**, 1126 (2021). [arXiv:2110.13518](#)
83. ATLAS collaboration, Measurement of the W -boson mass in pp collisions at $\sqrt{s} = 7$ TeV with the ATLAS detector. *Eur. Phys. J. C* **78**, 110 (2018). [arXiv:1701.07240](#)
84. CDF, D0 collaboration, Combination of CDF and D0 W -boson mass measurements. *Phys. Rev. D* **88**, 052018 (2013). [arXiv:1307.7627](#)
85. R. Bause, G. Hiller, T. Höhne, D.F. Litim, T. Steudtner, B-anomalies from flavorful $U(1)'$ extensions, safely. *Eur. Phys. J. C* **82**, 42 (2022). [arXiv:2109.06201](#)
86. B.C. Allanach, Going nowhere fast, Aeon online magazine (2018)